



HAL
open science

Comparison of the LSAST and MAPAS methods for ambiguity resolution on-the-fly

Christophe Macabiau

► **To cite this version:**

Christophe Macabiau. Comparison of the LSAST and MAPAS methods for ambiguity resolution on-the-fly. DSNS 1996, International Conference on Dependable Systems and Networks, May 1996, Saint-Petersburg, Russia. hal-00941973

HAL Id: hal-00941973

<https://enac.hal.science/hal-00941973v1>

Submitted on 18 Mar 2014

HAL is a multi-disciplinary open access archive for the deposit and dissemination of scientific research documents, whether they are published or not. The documents may come from teaching and research institutions in France or abroad, or from public or private research centers.

L'archive ouverte pluridisciplinaire **HAL**, est destinée au dépôt et à la diffusion de documents scientifiques de niveau recherche, publiés ou non, émanant des établissements d'enseignement et de recherche français ou étrangers, des laboratoires publics ou privés.

COMPARISON OF THE LSAST AND MAPAS METHODS FOR AMBIGUITY RESOLUTION ON-THE-FLY

Christophe MACABIAU
Ecole Nationale de l'Aviation Civile, Toulouse France
Presented at DSNS 96, Saint Petersburg, May 23 1996

ABSTRACT

The use of the pseudorange information contained within the GPS carrier phase measurements enables to achieve a high level of positioning accuracy. But full access to this accuracy in real time for dynamic applications, like aircraft landing, requires the resolution 'on-the-fly' of the intrinsic ambiguity of the phase measurements. This can be done using one of the numerous ambiguity searching procedures, among which ones are LSAST and MAPAS. These two methods can be seen as sequential tests of the same multiple hypotheses. They use distinct decision criteria, and this results in different implementation constraints, run-time capabilities and performances. Both of them show a similar behaviour when applied to clean data, but MAPAS appears to be more robust when using data affected by multipath. The comparison starts with a parallel presentation of the mathematical developments involved in the design of the two methods, then their practical advantages are reviewed and some results are shown of their application to clean and corrupted data.

1. INTRODUCTION

A high level of positioning accuracy can be obtained through the use of the very precise pseudorange information contained within the GPS signal carrier phase measurements. However, this pseudorange observation is biased because of the ambiguous nature of the carrier phase measurements. Full access to the value of the pseudorange requires the resolution of that bias, called the phase measurement ambiguity. The procedures performing this resolution in real time in dynamic applications are said to perform the ambiguity resolution 'on-the-fly'.

Many techniques for ambiguity resolution on-the-fly have been proposed so far, as summarized by Hatch and Euler (Hatch and Euler, 1994). These are for example the Ambiguity Function Method (AFM), described by Remondi (Remondi, 1991) and Mader (Mader, 1992), the Least Squares Ambiguity Search (LSAST), presented by Hatch (Hatch, 1991) and Lachapelle et al. (Lachapelle et al., 1992), the Fast Ambiguity Resolution Approach (FARA) described by Frei and Beutler (Frei and Beutler, 1990a), the Fast Ambiguity Search Filter (FASF) described by Chen (Chen, 1993), the optimized Cholesky

decomposition method, described by Landau and Euler (Landau and Euler, 1992), the integrated 'on-the-fly' technique described by Abiddin (Abiddin, 1991), the ambiguity transform method presented by Teunissen (Teunissen, 1994) and the Direct Integer Ambiguity Search (DIAS), presented by Ming and Schwarz (Ming and Schwarz, 1995).

The Maximum A Posteriori Ambiguity Search (MAPAS) method, jointly developed by SEXTANT AVIONIQUE, the Service Technique de la Navigation Aérienne (STNA) and the LTST, recently presented by the author (Macabiau, 1995), is another method for ambiguity resolution on-the-fly, which is based on the same principles as the LSAST.

These two procedures perform an active search of the value of the double differenced ambiguities of four particular satellites called the primary satellites. They both are multiple hypotheses sequential tests that process as many carrier phase measurements as necessary to isolate the best candidate in a predetermined set of three-integer combinations. However, the LSAST and MAPAS methods use different decision criteria to check the hypotheses: the LSAST is based on the weighted sum of the squared prediction errors obtained for the tested combination, while the MAPAS method uses the a posteriori probability of this candidate, conditionally on the prediction errors obtained for that candidate.

Thus these two algorithms have the same overall structure and only differ by the steps performing the calculation of the decision criterion. This results in different implementation constraints and running capabilities. Both of them can raise ambiguities in seconds when the data conforms to the mathematical model employed. However, they show different performances when applied to data affected by unmodeled noise such as multipath.

This paper first recalls the measurement model employed, then compares the theoretical principles of the LSAST and MAPAS methods and reviews their practical advantages, presents the results of their application, and draws a conclusion on this comparison.

2. MEASUREMENT MODEL

The data used by the LSAST and MAPAS methods are the linearized double differences of the carrier phase measurements.

The observed carrier phase measurements are tracked to keep a constant ambiguity. As described by Rocken (Rocken, 1988), a first order model of these measurements is as follows:

$$\Phi_i(k) = f(\Delta t_R(k) - \Delta t_{S_i}(k)) - \frac{D_i(k)}{\lambda} + f\tau_{ion} - f\tau_{trop} - N_i + b_i(k) + SA_i(k) + \varepsilon_{mult_i}(k) \quad (1)$$

where

- $\Phi_i(k)$ is the tracked carrier phase measurement of satellite i at epoch k
- f is the $L1$ carrier frequency and λ is the corresponding wavelength
- $\Delta t_R(k)$ and $\Delta t_{S_i}(k)$ are respectively the receiver and satellite time equivalent phase offset with respect to GPS time
- $D_i(k)$ is the geometrical distance between the satellite i and the receiver
- τ_{ion} and τ_{trop} are the ionospheric and tropospheric propagation delays
- N_i is the carrier phase measurement ambiguity
- $SA_i(k)$ is the perturbation introduced by the Selective Availability
- $\varepsilon_{mult_i}(k)$ is the phase measurement error induced by the multipath propagation of the signal
- $b_i(k)$ is the phase measurement noise. In the following, we assume that $b_i(k)$ is a discrete white gaussian noise, having zero mean and variance σ^2 .

The carrier phase tracking error $\varepsilon_{mult_i}(k)$ induced by multipath can cause loss of lock and may confuse the ambiguity resolution procedure because of the corresponding distortion of the signal in space, as this error is usually left unmodeled by the procedure.

For example, when the disturbing signal is one specular reflected ray, this term can be expressed as in (2), as presented by Lippincott et al. (Lippincott et al., 1996):

$$\varepsilon_{mult_i}(k) = \frac{1}{2\pi} \tan^{-1} \left(\frac{\alpha_i(k)R(\tau_i(k) - \Delta\tau_i(k))\sin(\theta_i(k))}{R(\tau_i(k)) + \alpha_i(k)R(\tau_i(k) - \Delta\tau_i(k))\cos(\theta_i(k))} \right) \quad (2)$$

where

- $\alpha_i(k)$ and $\theta_i(k)$ are the relative amplitude and phase terms with respect to the direct ray
- $\Delta\tau_i(k)$ is the relative delay of the reflected signal
- $\tau_i(k)$ is the time equivalent pseudorange measurement error
- R is the autocorrelation function of the C/A code

LINES OF CONSTANT PHASE: EARTH'S SURFACE SPECULAR MULTIPATH, A=0.45, EL=45 DEG

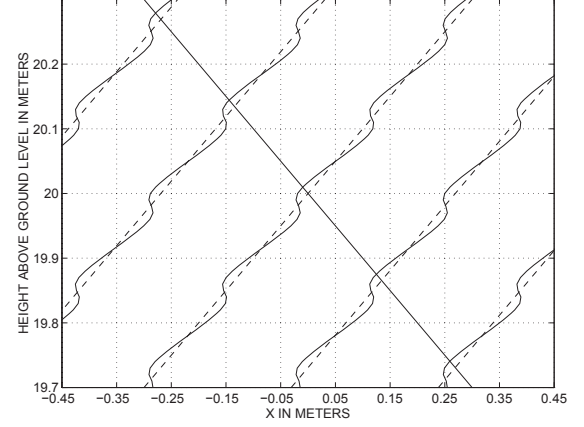


Figure 1: Example of the deformation of the lines of constant phase in space in the case of one specular reflected signal from the Earth's surface. We chose here $\alpha = 0.45$, for a satellite with an elevation angle of 45° . The curved continuous lines are the lines of constant phase resulting of the presence of the reflected signal, and are to be compared with the dashed lines in the ideal case. The straight line is the line of sight of the satellite.

In that simple case, having modeled the Earth's surface as a flat plate, the lines of constant phase in space may be distorted as shown in figure 1.

It can be shown that, in the case of one specular reflected ray, the error $\varepsilon_{mult_i}(k)$ is bounded, as

$$-0.25 < \varepsilon_{mult_i}(k) < 0.25$$

and will not cause a change in ambiguity, if left unmodeled. However, when several delayed signals interact, the error may be large enough to cause a full-cycle error and lead the ambiguity resolution procedure to raise wrong ambiguities.

In the next mathematical developments, we assume $\varepsilon_{mult_i}(k) = 0$. We will examine the effects of this term on the performances of the two methods in the last two chapters.

In order to eliminate the disturbing terms such as the atmospheric delays and the clock errors, double differences are formed using the measurements obtained by another receiver and all the n_k visible satellites.

These double differenced measurements are then linearized around a position estimate $\hat{X}(k)$, generally obtained by the use of LADGPS. A model of these quantities is

$$\Phi(k) = -C(k)\delta X(k) - N + B(k) \quad (3)$$

where

- $\Phi(k)$ is an $(n_k - 1) \times 1$ vector
- $\delta X(k)$ is the 3×1 vector of the position estimation error: $\delta X(k) = \hat{X}(k) - X(k)$

- N is the $(n_k - 1) \times 1$ vector of the double differenced ambiguities
- $C(k)$ is the $(n_k - 1) \times 3$ vector of the direction cosines
- $B(k)$ is the $(n_k - 1) \times 1$ vector of the phase measurement noise

The linear model given in (3) is the mathematical model used by both the LSAST and MAPAS methods.

3. COMMON PRINCIPLES OF LSAST AND MAPAS

The determination of the position is conditioned on the resolution of the double differenced ambiguity vector N . This resolution is done by testing thousands of possible values of N . These values are determined as the integer vectors associated with a position contained within a predefined search volume. This search volume is centered around the position estimate $\hat{X}(k)$, and its size depends on the uncertainty of that estimate.

The size of the trial set can be reduced if we note that only three of these ambiguities are independent in the noise-free model derived from (3). Thus the procedure looks for the best three-integer combination to be affected to the double differenced ambiguities of four particular satellites.

These satellites, called the primary satellites, are chosen according to their degree of visibility and their PDOP factor. They must stay visible as long as the resolution is not done, and their PDOP must not be too low nor too large, to guarantee a small number of candidates and a sufficient integrity. For example, the primary satellites can be chosen among the satellites of elevation greater than 7.5° as the satellites yielding the closet PDOP to the arbitrary reasonable value of 7.5.

Once the primary satellites are identified, the model (3) can be split into 2 systems of equations:

$$\Phi_P(k) = -C_P(k)\delta X(k) - N_P + B_P(k) \quad (4)$$

$$\Phi_S(k) = -C_S(k)\delta X(k) - N_S + B_S(k) \quad (5)$$

where the first system is the system of the primary satellites, and the other system is the system of the non primary satellites, called the secondary satellites.

The initial search set, denoted N_0 , can be built as the set of the three-integer combinations $N_{P_{abc}} = [a \ b \ c]^T$ associated with a position contained within the search volume using (4) as:

$$\hat{X}_{P_{abc}}(k) = -S_P(k)\Phi_P(k) - S_P(k)N_{P_{abc}}$$

where $S_P(k)$ is the pseudo-inverse of the primary system (4).

Thus, at each measurement epoch k , for each candidate $N_{P_{abc}} = [a \ b \ c]^T$ in the set N_k , the value of the associated secondary ambiguities $N_{S_{abc}}$ has to be determined.

This can be done using only the phase measurements at epoch k , although a more robust estimate can be elaborated using all of the previous measurements.

The first method is based on the assumption that, for the true solution $N_{P_{abc}} = N_P$, the vector

$$\tilde{N}_{S_{abc}}(k) = -\Phi_S(k) - C_S(k)\hat{X}_{P_{abc}}(k) \quad (6)$$

should be very close to N_S under normal low noise conditions. Thus we can choose to set

$$\hat{N}_{S_{abc}}(k) = \text{Round} \left[\tilde{N}_{S_{abc}}(k) \right]$$

But if the data is affected by multipath, $\hat{N}_{S_{abc}}(k)$ may be different from N_S .

A more robust estimate can be obtained if all the $\hat{N}_{S_{abc}}(k)$ are averaged over time. We will then have, for each secondary satellite i :

$$\hat{N}_{S_{abc_i}}(k) = \text{Round} \left[\sum_{j=k_i}^{k-1} \tilde{N}_{S_{abc_i}}(j) \right] \quad (7)$$

where k_i is the first epoch of lock on the signal transmitted by satellite i .

4. LSAST SPECIFIC STEPS

The estimate $\hat{N}_{S_{abc}}(k)$ is used by the LSAST to determine the phase measurements predictions for all the visible satellites, while the MAPAS method uses them to compute the phase measurements for the secondary satellites only.

Using the candidate ambiguity and its associated secondary ambiguity prediction, the LSAST computes the corresponding phase prediction error and its associated squared norm, then checks its validity against χ^2 values.

The complete ambiguity candidate is

$$\hat{N}_{abc}(k) = \begin{bmatrix} N_{P_{abc}} \\ \hat{N}_{S_{abc}}(k) \end{bmatrix}$$

This candidate is inserted in the complete model (3) to determine a prediction of the complete double differenced observations. We have

$$\hat{\Phi}_{abc}(k) = -C(k)\hat{X}_{abc}(k) - \hat{N}_{abc}(k)$$

with $\hat{X}_{abc}(k) = -S(k)\Phi(k) - S(k)\hat{N}_{abc}(k)$, where $S(k)$ is the pseudo-inverse of the complete model.

As presented by Leick for example (Leick, 1995), if $N_{P_{abc}} = N_P$, then

$$R_{L_{abc}}(k) = z_{abc}^T(k)\Sigma_c^{-1}(k)z_{abc}(k) \sim \chi_{n_k-4}^2$$

where $\Sigma_c(k)$ is the covariance matrix of the complete vector of observations $\Phi(k)$.

Thus $R_{L_{abc}}(k)$ can be checked against a likelihood threshold $\chi_{1-\alpha_L, (n_k-4)}$. But this test, called the local test, uses only the current prediction errors and may not be very reliable.

This problem can be overcome if we note that

$$R_{G_{abc}}(k) = \sum_{j=1}^k R_{L_{abc}}(j) \sim \chi_{N_T(k)}^2$$

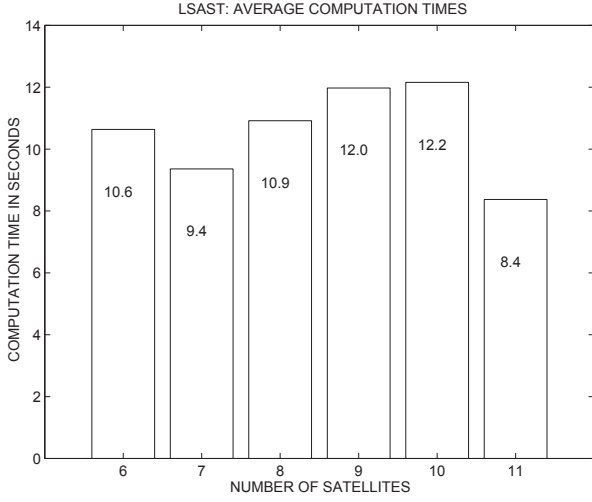


Figure 2: Average execution time of the LSAST simulation software as a function of the number of tracked satellites. The global average execution time is 11.2 s.

where $N_T(k) = \sum_{j=1}^k (n_j - 4)$. Thus we can build a more reliable test, based on all the previous residuals. This test is called the global test.

Improper solutions are progressively rejected from the search set, and the best solution is rapidly identified as the candidate associated with the lowest global residual. Confidence in the fact that this candidate is the correct one can be gained by performing the following approximate verification, as presented by Frei and Beutler (Frei and Beutler, 1990b):

$$\frac{R_G^*(k)}{R_{G_{abc}}^*(k)} \sim F_{\alpha_F, N_T(k), N_T(k)}$$

where $R_G^*(k)$ is the second lowest global residual at epoch k .

5. MAPAS SPECIFIC STEPS

The MAPAS method uses the predicted value of the secondary ambiguities to compute the associated secondary phase observations

$$\hat{\Phi}_{S_{abc}}(k) = -C_S(k) \hat{X}_{P_{abc}}(k) - \hat{N}_{S_{abc}}(k)$$

and the corresponding phase prediction errors $z_{S_{abc}}(k)$. Then, the value of the a priori probability density function is computed as

$$f(z_{S_{abc}}(k) | N_{P_{abc}} = N_P) = \frac{1}{2\pi^{\frac{n_k-4}{2}} \sqrt{\det(\Sigma(k))}} \times \exp\left(-\frac{1}{2} z_{S_{abc}}^\top(k) \Sigma^{-1} z_{S_{abc}}(k)\right)$$

where

$$\begin{aligned} \Sigma(k) = & C_S(k) S_P(k) \Sigma_{PP}(k) S_P(k)^\top C_S(k)^\top \\ & + \Sigma_{SS}(k) - C_S(k) S_P(k) \Sigma_{PS}(k) \\ & - \Sigma_{PS}(k)^\top S_P(k)^\top C_S(k)^\top \end{aligned}$$

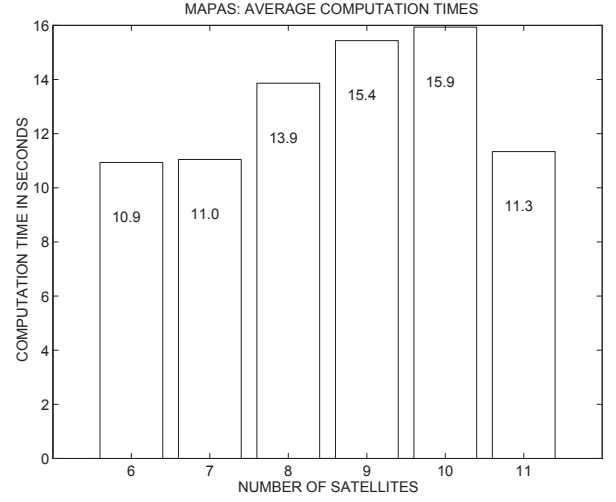


Figure 3: Average execution time of the MAPAS simulation software as a function of the number of tracked satellites. The global average execution time is 14.2 s.

$\Sigma_{PP}(k)$ and $\Sigma_{SS}(k)$ are the covariance matrices of the primary and the secondary observations.

The a posteriori probability is computed using Bayes' rule:

$$P[N_{P_{abc}} = N_P | (z_{S_{abc}}(k))] = \frac{f(z_{S_{abc}}(k) | N_{P_{abc}} = N_P)}{\sum_{abc \in N_k} f(z_{S_{abc}}(k) | N_{P_{abc}} = N_P)}$$

Thus, if the a posteriori probability of a candidate is lower than a predefined threshold, then it is rejected from the set and will not be tested for at the next epoch. If this probability is larger than a preset decision threshold, then this candidate is elected as the correct solution.

6. ALGORITHMS IMPLEMENTATION AND RUN-TIME CAPABILITIES

As we can see from the previous description, the two algorithms only differ by the steps dedicated to the evaluation of the criterion. This implies a difference in the implementation constraints and in the execution times.

The LSAST checks the squared norm of the residuals against values of the cumulative probability density functions of the χ^2 and F laws. These values may be needed for a few thousands of degrees of freedom if the procedure is long to converge, and for several error probabilities if the thresholds are tightened up over time. This may be heavy to handle, especially during the tuning period of the procedure.

The MAPAS method evaluates straight probabilities of occurrence, so the thresholds can be identified to the design error probabilities.

The execution times of two implementations of these procedures were compared on a statistical point of view

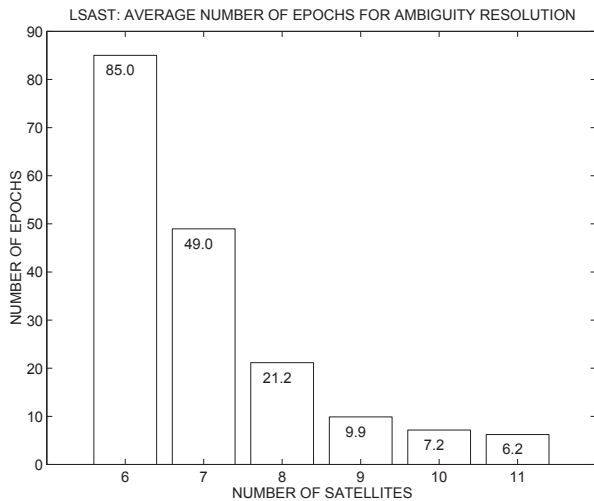


Figure 4: Average duration of the LSAST trials in seconds, as a function of the number of tracked satellites. The global average duration is 19.3 s.

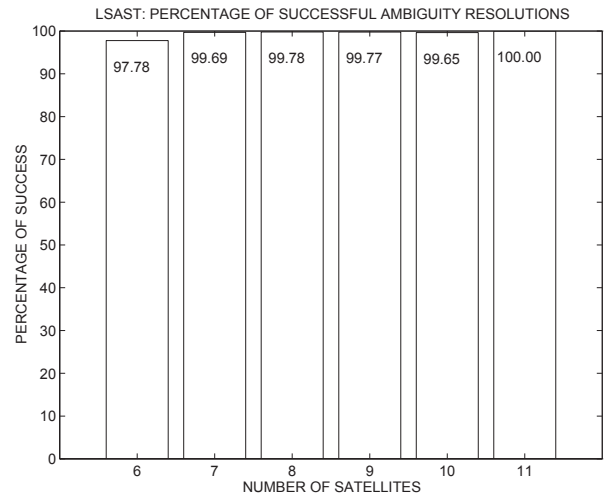


Figure 6: Percentage of successful LSAST trials as a function of the number of tracked satellites. The global percentage is 99.73%.

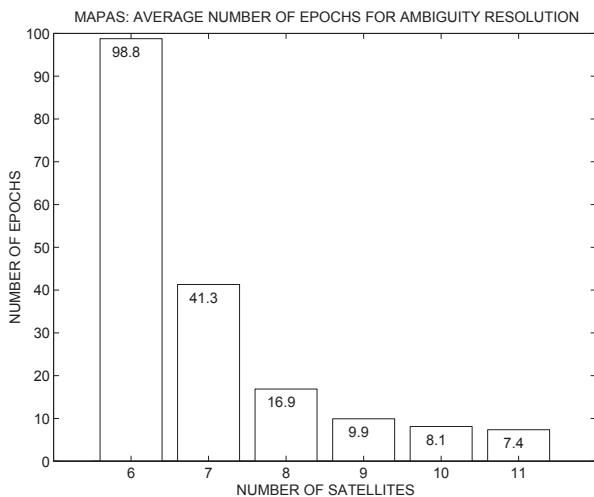


Figure 5: Average duration of the MAPAS trials in seconds, as a function of the number of tracked satellites. The global average duration is 17.8 s.

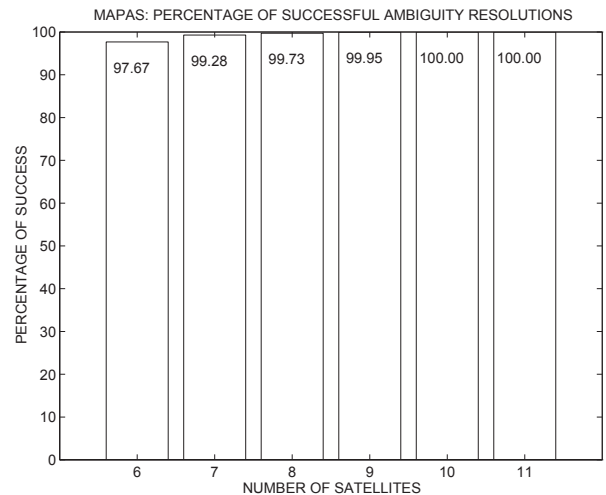


Figure 7: Percentage of successful MAPAS trials as a function of the number of tracked satellites. The global percentage is 99.76%.

(figures 2 and 3). The softwares were developed in ADA at the LTST and run on HP 712/80 workstations. This comparison is simply intended to give an order of magnitude of the difference between the execution times of the two procedures. Indeed, the computation are very specific to the implementation and the processing machines.

The ambiguity resolution trials are launched one after the other, using the satellite constellation visible from 0:00 a.m. till midnight. The phase data is generated every second for two receivers in a simulated dynamic configuration which is reset at the beginning of each trial. No multipath is assumed and the standard deviation of the measurement noise is set to $\sigma = 3.8$ mm.

7. PERFORMANCES ON REAL AND SIMULATED DATA

The performances of the two procedures are compared using clean data and data affected by multipath. For each trial we record the required number of samples and the success of the procedure. Simulated data are generated using a program providing theoretical single differences of phase for two receivers of given locations on Earth. One of the receivers is the reference station, of known location, and the other one is the moving receiver, following a certain simulated trajectory. The standard deviation of the phase measurement noise is set to $\sigma = 3.8$ mm. More than 10000 trials were performed in each case.

The two procedures are first run on simulated data conforming to the multipath-free model (figures 4, 5, 6, 7).

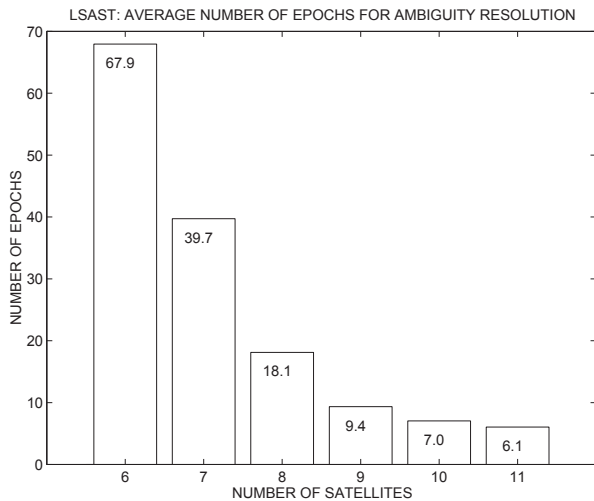


Figure 8: Average duration of the LSAST trials in seconds. The global average duration is 17.4 s.

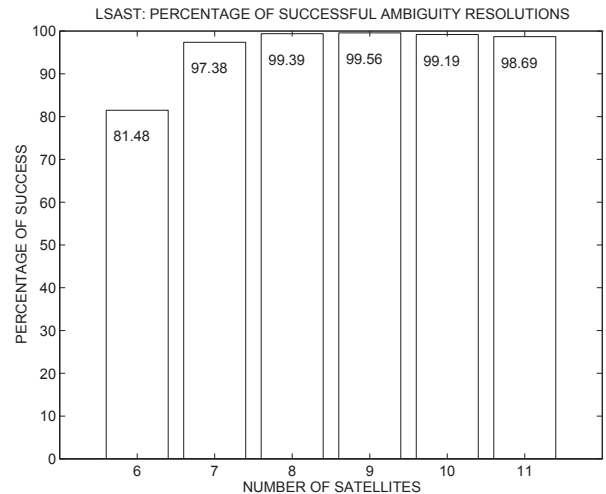


Figure 10: Percentage of successful LSAST trials. The global percentage is 98.92%.

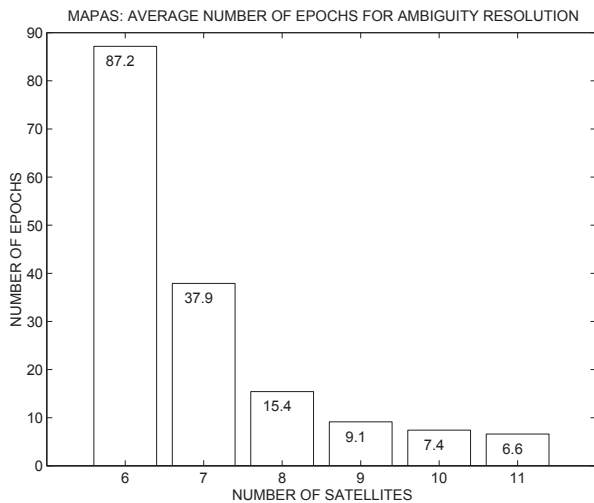


Figure 9: Average duration of the MAPAS trials in seconds. The global average duration is 16.4 s.

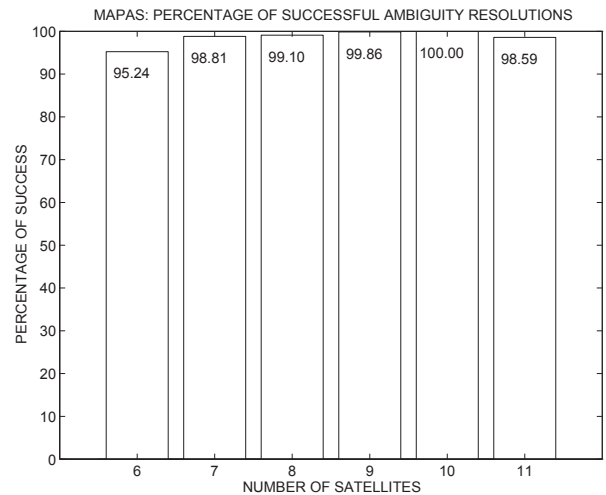


Figure 11: Percentage of successful MAPAS trials. The global percentage is 99.36%.

Then, specular multipath propagation on the Earth's surface is added, as it may be considered as the major contributing source of multipath during the final approach, as presented by Braasch (Braasch, 1992). The moving receiver is assumed to follow a runway approach path. Any reflected ray of path length difference greater than 1.5 C/A code chip is not considered.

To get a first idea of the influence of multipath, we set the reflected to direct signal voltage ratio to $\alpha = 0.1$, without any consideration of the nature of the ground, of the antenna pattern and of the autocorrelation attenuation (figures 8, 9, 10, 11). Thus equation (2) is used in its simplest form.

In a second stage, to get a better knowledge of the influence of the Earth's surface, the ground is modeled as wet soil, and a simple model of the receiving an-

tenna and of the receiver is implemented. The complex permittivity of the reflecting soil is set with $\varepsilon_r = 12.0$ and $\sigma_r = 0.4$. The receiving antenna is assumed to have a quasi omni-directional gain pattern with $G_r = \frac{1}{2}(1 + \sin(EL))$, and a 15 dB attenuation factor on left-hand circularly polarized waves with respect to the theoretical gain.

Equation (2) is used to model the measurement error induced by this ground reflection. The autocorrelation function employed has the ideal triangular shape, and an approximate value of the pseudorange measurement error is given by the weighted delay time of the reflected ray (figures 12, 13, 14, 15).

The success rate of the procedures can be improved by setting the a priori value of the standard deviation of the measurement noise to a larger value than the actual one, to take into account the effect of multipath. When this value is set to 7.6 mm, the global success rate for LSAST is 88.45%, and it is 95.36% for MAPAS.

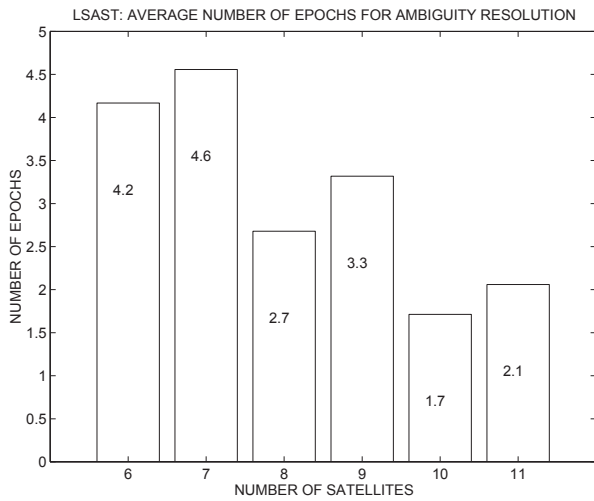


Figure 12: Average duration of the LSAST trials in seconds. The global average duration is 3.5 s.

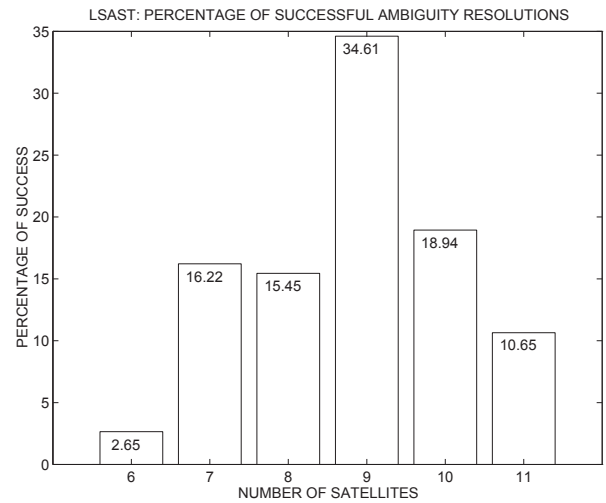


Figure 14: Percentage of successful LSAST trials. The global percentage is 20.97%.

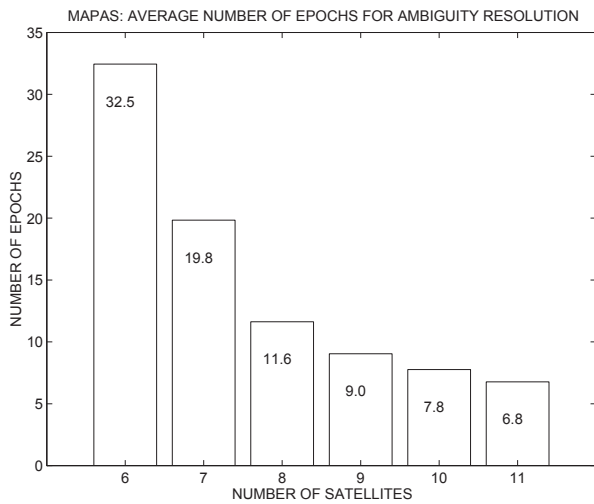


Figure 13: Average duration of the MAPAS trials in seconds. The global average duration is 13.9 s.

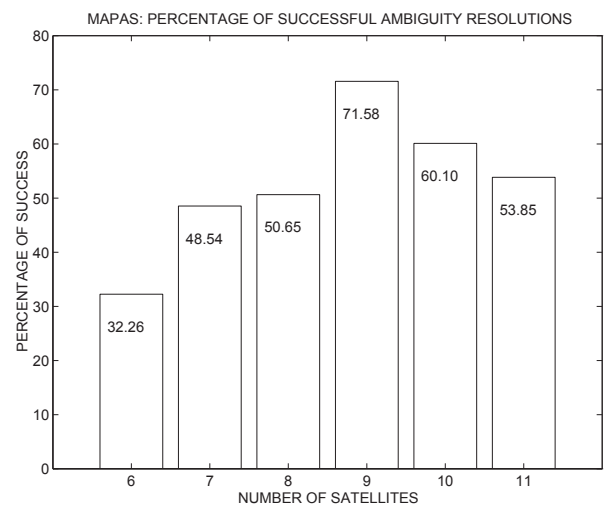


Figure 15: Percentage of successful MAPAS trials. The global percentage is 58.34%.

Finally, the two procedures are run on a 20 minute segment of real data severely affected by coloured noise such as multipath. These data were collected using an 8-channel SEXTANT AVIONIQUE NSS-100 GPS receiver at two points of known locations. The a priori value of the standard deviation of the measurement noise is set by using the variance of the phase tracking loop, giving an indication of the signal-to-noise ratio. Between 6 and 7 satellites were visible during this 20' segment.

	Number of trials in the 20' segment	Number of successful trials	Average duration of the trials
LSAST	12	1	74 s
MAPAS	6	3	190 s

8. CONCLUSION

The LSAST and MAPAS methods show similar performances when using clean data, but MAPAS seems to need more calculation power to raise the ambiguities.

Both of the procedures show significantly reduced performances when applied to data corrupted by coloured noise such as multipath, and this is a critical problem during the runway approach phase. However, MAPAS

appears to be more efficient in counteracting this perturbing effect.

Ongoing investigations aim at the characterization of this robustness, which needs further validation in other real situations.

ACKNOWLEDGEMENTS

The author wishes to thank the company SEXTANT AVIONIQUE for providing advices and technical assistance, as well as the technical services branch of the french civil aviation authority, the STNA, for supporting this research. He also wishes to thank Olivier Charleux for helping him in performing the LSAST study.

REFERENCES

- Abidin H. (1991)** *"New Strategy for 'On the fly' Ambiguity Resolution"*, proceedings of ION GPS-91, Albuquerque, September 11-13, The Institute Of Navigation, pages 875-886
- Braasch M.S. (1992)** *"Characterization of GPS Multipath Errors in the Final Approach Environment"*, proceedings of ION GPS-92, The Institute Of Navigation, Alexandria, Albuquerque, New Mexico, September 16-18, pages 383-394
- Chen D. (1993)** *"Fast Ambiguity Search Filter : A Novel Concept for GPS Ambiguity Resolution"*, proceedings of ION GPS-93, The Institute Of Navigation, Alexandria, Salt Lake City, Utah, pages 781-787
- Frei E. and Beutler G. (1990a)** *"Rapid Static Positioning based on the Fast Ambiguity Resolution Approach : The Alternative to Kinematic Positioning"*, proceedings of the Second International Symposium on Precise Positioning with GPS, GPS 90, Canadian Institute of Geomatics, Ottawa, Canada, September 3-7, pages 1197-1216
- Frei E. and Beutler G. (1990b)** *"Rapid Static Positioning based on the Fast Ambiguity Resolution Approach 'FARA': theory and results"*, Manuscripta Geodaetica, Volume 15 Number 6, pages 325-356
- Hatch R. (1991)** *"Instantaneous Ambiguity Resolution"*, proceedings of International Association of Geodesy Symposia 107 on Kinematic Systems in Geodesy, Surveying and Remote Sensing, New York, Springer-Verlag, pages 299-308
- Hatch R. and Euler H.J.(1994)** *"Comparison of several AROF kinematic techniques"*, proceedings of ION GPS-94, the Institute of Navigation, Alexandria, Salt Lake City, Utah, September 20-23, pages 363-370
- Lachapelle G., Cannon M.E. and Lu G. (1992)** *"High-Precision GPS Navigation with Emphasis on Carrier-Phase Ambiguity Resolution"*, Marine Geodesy, Volume 15 Number 4, pages 253-269
- Landau H. and Euler H.J. (1992)** *"On-The-Fly Ambiguity Resolution for Precise Differential Positioning"*, proceedings of ION GPS-92, The Institute of Navigation, Alexandria, September 16-18, Albuquerque, New Mexico, pages 607-613
- Leick A. (1995)** *"GPS Satellite Surveying"*, 2nd Edition, Wiley-Interscience
- Lippincott W.L., Milligan T.A. and Igli D.A. (1996)** *"Method for Calculating Multipath Environment and Impact on GPS Receiver Solution Accuracy"*, proceedings of ION National Technical Meeting, the Institute of Navigation, Alexandria, January 22-24, Santa Monica, California
- Macabiau C. (1995)** *"A new Concept for GPS Phase Ambiguity Resolution On-The-Fly: The Maximum A Posteriori Ambiguity Search (MAPAS) Method"*, proceedings of ION GPS-95, the Institute of Navigation, Alexandria, Palm Springs, September 12-15, California, pages 299-308
- Mader G. (1992)** *"Kinematic GPS Phase Initialization using the Ambiguity Function"*, proceedings of Sixth International Geodetic Symposium on Satellite Positioning, Columbus, Ohio, March 17-20, pages 712-719
- Remondi B.W. (1991)** *"Pseudo-kinematic GPS Results Using the Ambiguity Function Method"*, Journal of the Institute of Navigation, Volume 38 Number 1, pages 17-36
- Rocken C. (1988)** *"The Global Positioning System : A New Tool for Tectonic Studies"*, Ph.D. Dissertation, Universitat zu Koln, Cologne, West Germany.
- Teunissen P.J.G. (1994)** *"A New Method for Fast Carrier Phase Ambiguity Estimation"*, proceedings of PLANS-94, IEEE, New York, pages 562-573
- Wei M. and Schwarz K.P. (1995)** *"Fast Ambiguity Resolution Using an Integer Non Linear Programming Method"*, proceedings of ION GPS-95, the Institute of Navigation, Alexandria, Palm Springs, September 12-15, California, pages 1101-1110